Multireference Configuration Interaction Calculations of Electronic States of *N*-Methylformamide, Acetamide, and *N*-Methylacetamide

Jonathan D. Hirst,*,† David M. Hirst,‡ and Charles L. Brooks III†

Department of Molecular Biology, TPC-6, The Scripps Research Institute, 10550 North Torrey Pines Road, La Jolla, California 92037, and Department of Chemistry, University of Warwick, Coventry, CV4 7AL, U.K.

Received: February 25, 1997; In Final Form: April 25, 1997[⊗]

The electronic excited states of *N*-methylformamide (NMF), acetamide, and *N*-methylacetamide (NMA) have been computed using multireference configuration interaction methods. The amide spectra are dominated by the valence $\pi\pi^*$ state, computed for the different molecules to be in the range 7.46−8.21 eV. The Rydberg $\pi 3p_\pi$ state also features prominently in the spectra of acetamide and NMA. The computed vertical energies of the $\pi\pi^*$ transition appear to be 0.3−0.6 eV too high, suggesting that either the observed bands do not correspond to vertical transitions (in analogy to ethylene) or that the interaction between the valence and Rydberg states is artificially too strong. Our state-averaged calculations provide a balanced treatment, but may overestimate the valence−Rydberg interaction. Alternative CASPT2 calculations (Serrano-Andrés, L.; Fülscher, M. P. *J. Am. Chem. Soc.* **1996**, *118*, 12190−12199), which involved separate optimizations of different types of states and ignored the Rydberg−valence interaction, agreed well with the spectra of formamide and NMA but underestimated the $\pi\pi^*$ transition energy for NMF and acetamide. The Rydberg−valence interaction appears to be important in the amide spectra, and a completely adequate treatment is still to be found. Nevertheless, the MRCI calculations reproduce well the amide spectra and we report the computed electronic properties of NMA that provide a compact parameterization of the amide chromophore.

Introduction

In this paper, we describe the properties of the excited states and the electronic transitions of *N*-methylformamide (NMF), acetamide, and *N*-methylacetamide (NMA) as computed using modern quantum chemistry methods. NMA is widely used as a simple model of the peptide linkage in proteins. Recent studies have focused on the nature and influence of hydrogen bonding,[1−3] vibrational properties,[3−7] and isomerization between the cis and trans conformations.[6,8,9] Excited state properties of NMA, calculated using the semiempirical CNDO/S method, have been used to derive parameters for the calculation of the circular dichroism (CD) of proteins.[10] Our work here is, in part, directed toward improving these parameters. Below, we briefly summarize the most salient experimental and theoretical studies.

The ground state geometry of NMA has been determined using X-ray crystallography[11] and by gas-phase electron diffraction.[12] The ultraviolet absorption spectrum of NMA has been determined *in vacuo*,[13] in water, and in cyclohexane.[14] The absolute values of the extinction coefficients are not reported in the *in vacuo* study, presumably due to difficulties in the precise determination of concentration. The *in vacuo* $\pi\pi^*$ transition energy is 6.81 eV. The $\pi\pi^*$ transition energy is reported to be 6.67 eV in water and 6.74 eV in cyclohexane. The respective oscillator strengths are 0.30 and 0.17. The $n\pi^*$ transition is less reliably described but, in both water and nonpolar solvents, occurs at 5.54 eV, with an oscillator strength on the order of 0.0025 and a transition dipole of 0.12 D.

Early theoretical work used self-consistent field (SCF) and configuration interaction (CI) methods to calculate the vertical excitation energies of NMA.[15] These calculations estimated the $n\pi^*$ transition energy to be 5.85 eV and concluded that the broad V band observed in the experimental absorption spectrum[13] arises from strongly mixed $\pi\pi^*$, $\pi 3p_\pi$, and n3p configurations. The conclusions about the V band were somewhat qualitative, because these calculations did not take account of the large relaxation and correlation effects.

Analogous experimental data are available for NMF and acetamide. The ground state geometries of NMF and acetamide have been determined by gas-phase electron diffraction,[16,17] and their ultraviolet absorption spectra have been measured *in vacuo*[13] and in solution.[14] A recent paper on the polarized crystal spectra of propanamide and *N*-acetylglycine[18] has provided the most definitive data to date on the direction of the $\pi\pi^*$ transition dipole moment in amides. The $\pi\pi^*$ transition in propanamide was observed at 6.70 eV and is polarized at −35° relative to the C−O axis (positive angles were measured toward the N atom). In this paper, Clark also succinctly summarizes other experimental data on the amide chromophore.

The advent of methods that account for extensive electron correlation has prompted us to examine the excited states of amides. Previously, we have performed excited state calculations on formamide using multireference configuration interaction (MRCI) methods.[19] The $n\pi^*$ transition was calculated to be at 5.85 eV (the experimental energy is 5.65 eV) and the $\pi\pi^*$ transition at 7.94 eV (the experimental energy is 7.32 eV). A number of other states with significant intensity were calculated to fall within the V band of the experimental spectrum. This work suggested that a number of issues are important in the calculation of the excited states of amides, in particular, the unbiased treatment of several states, correlation effects, and the use of appropriate diffuse functions to describe Rydberg states. Experimental and other theoretical studies on formamide are discussed in our previous paper.

An issue of some concern has been the treatment of Rydberg states and their interaction with valence excited states. The importance of a balanced treatment has been discussed in some detail by Roos and co-workers,[20] who have argued that care

* Address correspondence to this author. Tel: 619-784-9290. Fax: 619-784-8688. E-mail: jhirst@scripps.edu.
† The Scripps Research Institute.
‡ University of Warwick.
⊗ Abstract published in *Advance ACS Abstracts,* June 1, 1997.

S1089-5639(97)00675-0 CCC: $14.00

must be taken to avoid artificial mixing between Rydberg and valence excited states. Artificial mixing may arise as follows. Effects of dynamic correlation may be significant for some valence excited states, but they are usually smaller for Rydberg states. If this is the case, then the reference wave function for the valence excited state may have a larger energy than one or several Rydberg states, which in turn may give rise to an exaggerated interaction between the valence and Rydberg states, causing the valence state orbitals to be too diffuse. This may be difficult to correct in a subsequent CI calculation.

The electronic spectrum of ethylene and various calculations of the electronic states of ethylene have illustrated the importance of mixing between Rydberg and valence states. The experimental spectrum is dominated by an intense $\pi\pi^*$ excitation, with the band maximum at 7.66 eV. MRCI calculations[21] placed the vertical transition at 7.94 eV. The difference between the band maximum and the calculated vertical transition energy has been ascribed to the twisting of the $\pi\pi^*$ state. Vibrational analysis of the electronic spectrum of ethylene based on SCF-CI calculations[22] has placed the most probable vibrational transition energy at 7.89 eV, 0.4 eV below the computed vertical transition energy. More recent MRCI calculations[21] are in general accord with this conclusion, estimating this difference to be 0.28 eV. CASPT2 calculations[23] gave a vertical transition energy of 8.4 eV. However, it was anticipated that it would be difficult to achieve a good result for this state with second-order perturbation theory because of the valence−Rydberg mixing.

An inadequate basis set may lead to artificial mixing, and thus it is important to use a basis set that can provide a good representation of Rydberg orbitals. Two approaches have been adopted for representing Rydberg states. One is to place diffuse orbitals on each heavy atom. This approach was used, for example, in calculations of linear polyenes (including ethylene),[21,23] MRCI studies of formaldehyde,[24] and MRCI calculations on formamide.[19] We have continued to use this approach. An alternative is to place diffuse functions at the average charge centroid of the cation. This approach has been widely used in CASPT2 calculations, including calculations on formaldehyde[25] and acetone.[26] The approach reduces the number of basis functions and was introduced in a theoretical study of cyclic pentadienes,[27] where the use of diffuse functions on every heavy atom made it impossible to locate the valence excited states. Such problems were not encountered in our MRCI calculations.

Artificial mixing between Rydberg and valence states may also occur if a higher Rydberg state not included in the active space is nearly degenerate (in the zeroth-order Hamiltonian) to a given excited state.[20] This mixing may be avoided by deleting the Rydberg orbital from the molecular orbital basis, or by including it in the active space.[27,28] As has been noted,[29] deleting the Rydberg orbitals clearly involves the neglect of any possible real interaction between Rydberg and valence excited states. If valence states are computed with the Rydberg orbitals deleted, their transition properties are usually computed with respect to a ground state computed with the Rydberg orbitals deleted.

In our calculations on formamide, we placed diffuse functions on each heavy atom. The valence $\pi\pi^*$ transition and the $\pi 3p_\pi$ transition to the Rydberg $3p_\pi$ orbital clearly interacted. Calculations were performed with and without the Rydberg $3p_\pi$ orbital in the active space. The inclusion of the Rydberg $3p_\pi$ orbital noticeably reduced the intensity of the $\pi\pi^*$ transition, although this was compensated somewhat by the intensity of the $\pi 3p_\pi$ transition itself. However, it is difficult to say whether this mixing is artificial or real. The computed vertical transition energy of the $\pi\pi^*$ transition was 0.6 eV above the experimentally observed band maximum. Ultraviolet resonance Raman experiments on NMA[6,30] and geometry optimizations of the $\pi\pi^*$ state of formamide and NMA[31] strongly indicate that the $\pi\pi^*$ excited state of formamide is twisted, and as in the case of ethylene, this may account for the discrepancy between the MRCI calculation of the transition energy and the experimental band maximum. If this is the case, then real mixing between the valence and Rydberg states would be consistent with the experimental spectrum—the intense V band would be attributed mainly to the $\pi\pi^*$ transition, with a lesser but nevertheless significant contribution from the $\pi 3p_\pi$ transition. Given that no artifacts were obvious from the protocol used for formamide, we have continued to use this procedure in this study.

TABLE 1: Geometries Used in This Study[a]

internal coordinate	NMF	acetamide	NMA
r_{CN}	1.3577 (1.366)	1.3693 (1.3180)	1.3655 (1.386)
r_{CC}	N/A[b]	1.5137 (1.519)	1.5144 (1.520)
r_{CO}	1.2334 (1.219)	1.2334 (1.220)	1.2376 (1.224)
r_{NCt}	1.4541 (1.459)	N/A	1.4528 (1.468)
r_{NHb}	1.0072 (1.125)	1.0070 (1.022)	1.0066 (1.106)
r_{NHc}	N/A	1.0046 (1.022)	N/A
r_{CHa}	1.0995 (1.125)	N/A	N/A
r_{CtHg}	1.0864 (1.114)	N/A	1.0869 (1.106)
$r_{CtHh} = r_{CtHi}$	1.0887 (1.114)	N/A	1.0889 (1.106)
r_{CHd}	N/A	1.0851 (1.124)	1.056 (1.106)
$r_{CHe} = r_{CHf}$	N/A	1.0901 (1.124)	1.0902 (1.106)
$\angle NCO$	123.9872 (124.0)	121.8963 (122.0)	121.4923 (121.8)
$\angle CCO$	N/A	123.1894 (123.0)	123.1478 (124.1)
$\angle CCN$	N/A	114.9144 (115.1)	115.3599 (114.1)
$\angle CNH_b$	118.6690 (118.7)	112.4182 (120.0)	119.4542 (110.0)
$\angle CNC$	121.1169 (121.4)	N/A	120.8194 (119.4)
$\angle NCH_a$	113.2028 (112.7)	N/A	N/A
$\angle NC_tH_g$	108.5252	N/A	108.4345 (110.4)
$\angle NC_tH_h = \angle NC_tH_i$	110.4342	N/A	110.5665 (110.4)
$\angle CCH_d$	N/A	108.5771 (109.8)	108.4537 (110.4)
$\angle CCH_e = \angle CCH_f$	N/A	110.5092 (109.8)	110.6884 (110.4)
τ_{HCNC}	59.9399	N/A	59.8989
τ_{HCCN}	N/A	59.9253	60.0812

[a] Bond lengths are in angstroms; angles and dihedrals are in degrees. Experimental data are in parentheses. [b] N/A = not applicable.

Computational Details

Excited state calculations of NMF, acetamide, and NMA were performed with the MOLPRO suite of programs.[32] Ground state and excited state energies and permanent and transition dipole and quadrupole moments were computed using the internally contracted MRCI procedure.[33,34] The MRCI calculations used the multiconfiguration SCF (MCSCF) orbitals from state-averaged complete-active-space SCF (CASSCF)[35,36] calculations. The procedure is similar to that used for excited state calculations on formamide.[19] The molecular orbitals thus obtained are not biased toward any particular electronic state and should be a good starting point for MRCI calculations of excited states. All configurations with a norm ≥ 0.05 in any state in the CASSCF wave function were taken as reference configurations for the MRCI calculations.

The geometries used in these calculations (see Table 1) were taken from geometry optimizations, with C_s symmetry, at the MP2 level (second-order Møller−Plesset perturbation theory[37]), using a 6-31+G** basis set. The restriction of C_s symmetry maintains planarity of the amide group and has been recently justified in detail.[38] The labeling and final coordinate systems are defined in Figure 1. The CHONC skeleton of NMF was planar with the methyl group cis to the oxygen. For NMA, we use the geometry with the two methyl groups trans to each other.

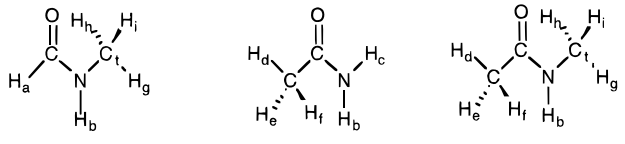

I **II** **III**

Figure 1. NMF (**I**), acetamide (**II**), and NMA (**III**): structure and labeling. All heavy atoms lie in the *xy* plane. The molecules were oriented such that the origin was the center of mass and the axes were the eigenvalues of the inertia tensor. The coordinate system of the dipole and quadrupole moments we report later are defined by the *xy* coordinates in atomic units of the amide C, N, and O atoms: for NMF, C (−1.431 434, 0.960 046), N (1.122 672, 1.203 479), O (−2.545 117, −1.087 459); for acetamide, C (0.080 266, −0.154 830), N (1.582 802, 1.951 841), O (0.976 214, −2.306 539); for NMA, C (−0.902 023, −0.187 822), N (1.208 416, 1.296 973), O (−0.753 709, −2.521 839).

TABLE 2: Exponents of the Diffuse Functions

type	atom	exponents	
s	H	0.03600	
p	H	0.03600	
s	C	0.01752	0.04370
s	N	0.02100	0.05320
s	O	0.02400	0.06080
p	C	0.01575	0.03990
p	N	0.01875	0.04750
p	O	0.02100	0.05320

These geometry optimization calculations, which were performed using the package Gaussian94,[39] essentially reproduced the experimental geometries[12,16,17] (shown in parentheses in Table 1).

The choice of basis set has been guided by our previous calculations on formamide. The use of one, two, or three sets of diffuse functions had little quantitative effect on the calculated spectrum of formamide. No changes to the calculated spectrum were apparent upon the inclusion of diffuse d functions, the use of 6-311++G**, or the correlation consistent valence double and triple zeta basis sets. Thus, negligible differences were seen for several basis sets of reasonable quality. An important feature, however, was the use of exponents for the diffuse functions appropriate for Rydberg states. Here, we use a 6-31+G** split-valence basis set (with spherical harmonic d functions),[40] with the exponents for the diffuse functions suggested by Dunning and Hay for Rydberg states.[41] These exponents are in Table 2. We have not explored effects due to basis set as closely as we did for formamide, but several calculations not reported here indicate that our observations for formamide are valid for the molecules in this study. For example, the inclusion of diffuse d functions did not change the computed spectrum of NMA.

In order to investigate the interaction between valence and Rydberg states, we have performed calculations with a number of different active spaces. The electronic ground states of NMF/acetamide (these two molecules are isoelectronic) and NMA are respectively $(1a')^2...(13a')^2(1a'')^2(2a'')^2(3a'')^2$ and $(1a')^2...(16a')^2(1a'')^2...(4a'')^2$. In all the active spaces, for NMF and acetamide, the two highest occupied π orbitals, the highest occupied a′ orbital (the lone pair on oxygen, *n*), the lowest unoccupied a′ orbital (the Rydberg 3s orbital), and the lowest unoccupied a″ orbital (the π^* orbital—although the ordering of the a″ virtual orbitals depends on the active space) were included; the occupied orbitals below this were treated as closed in the MCSCF calculations and as core orbitals in the MRCI calculations. Analogous active spaces were considered for NMA, except that the lowest two occupied a″ orbitals were treated as closed. Thus, six active electrons were considered for each molecule. Due to computational limitations, it was impossible to consider active spaces with all the Rydberg p and d orbitals, so we systematically explored the inclusion of these orbitals with a series of active spaces. Apart from the interaction between the $\pi\pi^*$ and $\pi 3p_\pi$, the details of the active space were not expected to be particularly important, on the basis of our previous study of formamide.

Many calculations gave quantitatively very similar results, and so we present detailed data for a set of representative calculations on each molecule: for two "small" active spaces and one "large" active space. We adopt the following notation for describing an active space: (*i*, *j*; *m*, *n*), where *i* is the number of closed orbitals of a′ symmetry, *j* is the number of closed orbitals of a″ symmetry, *m* is the sum of the active and closed orbitals of a′ symmetry, and *n* is the analogous sum for the orbitals of a″ symmetry. Thus, for NMF and acetamide we consider calculations with active spaces (12, 1; 14, 4), (12, 1; 14, 5), and (12, 1; 16, 7), and for NMA we consider the active spaces (15, 2; 17, 5), (15, 2; 17, 6), and (15, 2; 19, 8). These calculations represent "minimal" calculations with and without the Rydberg $3p_\pi$ orbital, and the largest calculations that we could do including the Rydberg 3p orbitals of a′ and a″ symmetry and the Rydberg 3d a″ orbitals. Depending on the size of the active space, different numbers of states were computed at the MRCI level, using the projection procedure of Knowles and Werner.[42] For the smallest active space, three A′ states and two A″ states were computed; for the largest active space, six A′ and five A″ states were computed (as reflected in Tables 3−5). Initial orbitals were obtained from state-averaged MCSCF calculations over the same number of states to be computed at the MRCI level. For the large active space MCSCF calculations, there were ∼2500 configurations for each state. In the following results and discussion sections we focus on the large active space calculations and indicate the differences between them and the smaller active space calculations.

Results

In Figure 2, we show the electronic absorption spectra of NMF, acetamide, and NMA adapted from the original experimental work[13] and the calculated vertical transitions from CASPT2 calculations[38] and from our MRCI calculations using the small and large active spaces. The intensities of the experimental data are arbitrary, and the calculated oscillator strengths have been arbitrarily scaled by a constant factor for the figure. The detailed results of the calculations on NMF, acetamide, and NMA are provided in Tables 3, 4, and 5, respectively. The spectra of each molecule are discussed below.

For the MRCI calculation of NMF with an active space of (12, 1; 16, 7), there were about 287 000 contracted configurations for the A′ states and about 270 000 contracted configurations for the A″ states. The computed spectrum is dominated by the intense (oscillator strength, $f = 0.37$) $\pi\pi^*$ transition at 7.70 eV. The $\pi\pi^*$ state was found to be the sixth A′ state, with the intervening A′ states n3s, $n3p_x$, $n3p_y$, and $\pi 3p_\pi$. The 1 A″ state is the π3s state, and the higher A″ states are $n\pi^*$, $\pi 3p_x$, $\pi 3p_y$, and $n3p_\pi$. The A″ states all have little intensity. The broad nature of the experimental spectrum makes it difficult to locate definitively the Rydberg transitions. Nevertheless, below the band maximum at 7.4 eV, peaks are observed in the experimental spectrum at 6.45, 7.0, 7.2, and 7.3 eV which correspond well to the computed Rydberg transition energies at 6.37, 6.93, 7.18, and 7.26 eV. Serrano-Andrés and Fülscher[38] have suggested that the peak at 7.0 eV is the $\pi\pi^*$ transition and that the band maximum at 7.4 eV is a Rydberg n3p

TABLE 3: MRCI Energies and Properties of NMF[a]

active space	(12, 1; 14, 4)			(12, 1; 14, 5)			(12, 1; 16, 7)		
	energy	perm moment	trans moment	energy	perm moment	trans moment	energy	perm moment	trans moment
1 ^{1}A′ (G.S.)	0[b]	(3.59, −2.97)		0[c]	(3.74, −2.93)		0[d]	(3.88, −2.86)	
2 ^{1}A′ (n3s)	6.69	(−1.63, 6.46)	(0.22, 0.60)	6.50	(−1.79, 6.74)	(0.09, 0.65)	6.37	(−0.15, 6.45)	(0.04, 0.66)
3 ^{1}A′ (π3p$_\pi$)		N/A[e]		7.05	(1.89, 0.58)	(−0.43, 0.79)	6.93	(1.60, 0.78)	(−0.52, 0.80)
4 ^{1}A′ (n3p)		N/A			N/A		7.18	(1.82, −5.66)	(−0.78, −0.60)
5 ^{1}A′ (n3p)		N/A			N/A		7.26	(0.93, 3.21)	(−0.40, 0.81)
6 ^{1}A′ ($\pi\pi$*)	7.84	(5.57, −1.84)	(3.31, −1.54)	7.82	(6.00, −1.92)	(3.30, −1.47)	7.70	(3.01, −0.93)	(3.17, −1.53)
1 ^{1}A″ (π3s)	6.10	(−0.96, 6.27)	−0.57	5.90	(−0.28, 4.68)	−0.46	5.78	(−1.37, 6.42)	−0.55
2 ^{1}A″ (nπ*)	5.90	(2.01, −1.12)	−0.17	5.91	(1.48, 0.62)	−0.44	5.94	(2.30, −0.86)	−0.16
3 ^{1}A″ (π3p)		N/A			N/A		6.82	(−1.13, −5.89)	0.48
4 ^{1}A″ (π3p)		N/A			N/A		7.02	(7.72, 3.15)	0.48
5 ^{1}A″ (n3p$_\pi$)		N/A		7.46	(0.37, 1.13)	−0.34	7.33	(0.02, 1.40)	−0.31

[a] Assignments are given in parentheses after the state label. Data from calculations using three different active spaces are presented. Excited state energies are given in electron volts relative to the ground state. Permanent and transition dipole moments are given in debye. The coordinate system is defined in the legend to Figure 1. The A′ states have transition dipole moments with two in-plane components; the A″ states have a single component, perpendicular to the plane. G.S. = ground state. [b] Ground state energy = −208.083 579 hartrees. [c] Ground state energy = −208.079 910 hartrees. [d] Ground state energy = −208.078 212 hartrees. [e] N/A = not applicable.

TABLE 4: MRCI Energies and Properties of Acetamide[a]

active space	(12, 1; 14, 4)			(12, 1; 14, 5)			(12, 1; 16, 7)		
	energy	perm moment	trans moment	energy	perm moment	trans moment	energy	perm moment	trans moment
1 ^{1}A′ (G.S.)	0[b]	(−1.15, 4.35)		0[c]	(−1.31, 4.47)		0[d]	(−1.80, 4.28)	
2 ^{1}A′ (n3s)	6.68	(−3.84, −4.42)	(−0.77, 0.10)	6.50	(−4.28, −4.94)	(−0.72, 0.15)	6.30	(−3.50, −3.35)	(−0.93, −0.02)
3 ^{1}A′ (π3p$_\pi$)		N/A[e]		7.13	(−0.84, 1.18)	(−0.53, −2.25)	7.00	(0.68, 1.84)	(−0.45, −2.15)
4 ^{1}A′ (n3p)		N/A			N/A		7.24	(−2.54, −1.38)	(0.72, −0.17)
5 ^{1}A′ (n3p)		N/A			N/A		7.30	(−1.26, −0.46)	(−0.13, −0.85)
6 ^{1}A′ ($\pi\pi$*)	7.75	(0.26, 3.90)	(−0.61, −3.31)	8.37	(2.07, 2.89)	(0.46, 2.10)	8.21	(1.72, 4.14)	(−0.43, −2.35)
1 ^{1}A″ (π3s)	6.37	(−3.04, −3.37)	−0.91	6.07	(−3.41, −3.63)	−1.01	5.92	(−3.04, −3.78)	−0.97
2 ^{1}A″ (nπ*)	5.89	(−0.45, 1.66)	0.12	5.93	(−0.66, 1.52)	0.00	6.02	(−0.98, 1.30)	−0.09
3 ^{1}A″ (π3p)		N/A			N/A		7.11	(−4.42, −1.42)	−0.06
4 ^{1}A″ (π3p)		N/A			N/A		7.32	(2.71, 5.03)	−0.36
5 ^{1}A″ (n3p$_\pi$)		N/A		7.59	(−1.51, −1.19)	−0.18	7.39	(0.71, 0.29)	−0.04

[a] Units and conventions as for Table 3. [b] Ground state energy = −208.100 825 hartrees. [c] Ground state energy = −208.094 773 hartrees. [d] Ground state energy = −208.090 872 hartrees. [e] N/A = not applicable.

TABLE 5: MRCI Energies and Properties of NMA[a]

active space	(15, 2; 17, 5)			(15, 2; 17, 6)			(15, 2; 19, 8)		
	energy	perm moment	trans moment	energy	perm moment	trans moment	energy	perm moment	trans moment
1 ^{1}A′ (G.S.)	0[b]	(0.06, 4.59)		0[c]	(0.88, 4.69)		0[d]	(0.92, 4.83)	
2 ^{1}A′ (n3s)	6.67	(−1.59, −6.77)	(−0.43, 0.06)	6.43	(−1.64, −6.88)	(−0.47, 0.07)	6.16	(−0.42, −4.98)	(−0.66, 0.04)
3 ^{1}A′ (π3p$_\pi$)		N/A[e]		6.74	(0.54, −0.21)	(−0.45, −1.45)	6.53	(1.14, −0.01)	(−0.57, −1.65)
4 ^{1}A′ (n3p)		N/A			N/A		6.89	(−1.19, 2.04)	(0.54, −0.36)
5 ^{1}A′ (n3p)		N/A			N/A		7.04	(−3.04, −0.77)	(0.64, 0.16)
6 ^{1}A′ ($\pi\pi$*)	7.62	(3.30, 2.89)	(−1.81, −2.86)	8.05	(2.25, 4.87)	(−1.98, −2.25)	7.46	(−3.85, 5.78)	(−1.21, −1.67)
1 ^{1}A″ (π3s)	6.02	(−0.36, −5.39)	−0.55	5.76	(−0.43, −5.45)	−0.58	5.56	(−0.73, −5.92)	−0.66
2 ^{1}A″ (nπ*)	5.96	(0.60, 1.71)	0.15	5.99	(0.64, 1.64)	0.19	6.14	(0.75, 1.02)	0.10
3 ^{1}A″ (π3p)		N/A			N/A		6.64	(−0.39, 6.58)	0.68
4 ^{1}A″ (π3p)		N/A			N/A		6.77	(0.03, −0.78)	−0.22
5 ^{1}A″ (n3p$_\pi$)		N/A		7.24	(−1.19, −0.93)	−0.04	7.02	(−2.51, 1.80)	−0.05

[a] Units and conventions as for Table 3. [b] Ground state energy = −247.127 994 hartrees. [c] Ground state energy = −247.122 875 hartrees. [d] Ground state energy = −247.119 070 hartrees. [e] N/A = not applicable.

transition. However, this interpretation is not consistent with our calculations or with their interpretation of the other amide spectra. The computed nπ* vertical transition energy is 5.94 eV. Although some quantitative differences were seen with smaller active spaces, and obviously less Rydberg states were computed, the smaller active space calculations gave results that were qualitatively similar to those from the large active space calculation.

For acetamide with an active space of (12, 1; 16, 7), the number of configurations in the MRCI calculation was ∼250 000 for the A′ states and ∼240 000 for the A″ states. The computed spectrum for acetamide is more similar to that of formamide than to NMF. There are two transitions of similar intensity, the transition to the Rydberg 3 A′ (π3p$_\pi$) state at 7.00 eV (f = 0.13) and to the valence 6 A′ ($\pi\pi$*) state at 8.21 eV (f = 0.18). The experimental spectrum is quite featureless, and there are no discernible peaks below the band maximum at 7.5 eV. In the small active space calculation, as was the case for formamide, the π3p$_\pi$ state is not seen (as expected) and the $\pi\pi$* transition has a large intensity (f = 0.33). The other Rydberg transitions have weak intensity. The nπ* state appears at 5.92 eV.

For the NMA calculation with an active space of (15, 2; 19, 8), there were ∼490 000 contracted configurations in the MRCI calculations of A′ states and ∼390 000 for the A″ states. The spectrum is similar to that of acetamide, but the $\pi\pi$* (at 7.46 eV, f = 0.12) and π3p$_\pi$ (at 6.53 eV, f = 0.08) transitions are 0.5−0.7 eV lower in energy. Their intensities are comparable to those of acetamide. Again, in the small active space calculation, the π3pπ state is not seen, and the $\pi\pi$* transition has

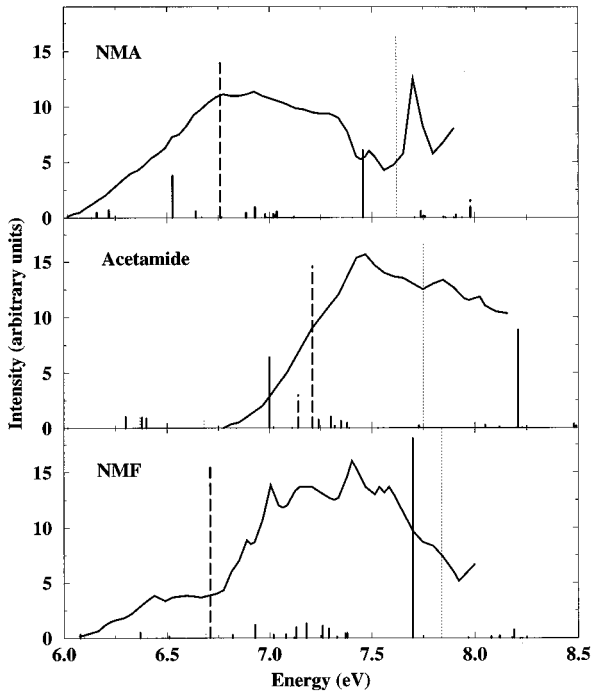

Figure 2. Experimental and calculated amide spectra. The solid black curve is adapted from the reported experimental data.[13] The solid vertical lines are the computed vertical transitions from MRCI calculations using the large active space. The dotted vertical lines are from MRCI calculations using the small active space. The dashed vertical lines are taken from CASPT2 calculations.[38]

an oscillator strength of 0.33. The nπ* transition appears at 6.14 eV.

As alluded to in the Introduction, part of our interest in the electronic states of NMA arises from the use of parameters describing the properties of these states and transitions between them in calculations of the circular dichroism spectra of proteins. The three major states that play a role in the circular dichroism of proteins are the ground state, the nπ* state, and the $\pi\pi$* state. Other states are also believed to be important, but the exact nature of the states and their role is less well established, so we focus on the three major states.

In their widely cited theoretical study of the circular dichroism of polypeptide helices,[10] Manning and Woody presented parameters used in the matrix method[43] to describe the permanent and transition properties of the amide electronic states expected to be relevant to the circular dichroism of proteins. The parameters are mainly sets of monopole charges to represent charge distributions and were derived from CNDO/S calculations on NMA. We have computed the resulting dipole and quadrupole moments and summarize these and the other parameters in Table 6. In Table 7 we report the properties computed from the MRCI wave function. Although the permanent properties of the excited states do not appear in the matrix method formulation of protein circular dichroism calculations, they do appear in the first-order perturbation method,[44−46] and so in Table 8 we have reported those properties. In condensed phases Rydberg states may not appear, in which case the parameters from the calculation in which the Rydberg orbitals are not included in the active space may be a more appropriate description of the amide chromophore in proteins. The suitability of these gas-phase parameters for describing the hydrogen-bonded amide chromophore in proteins in aqueous solution remains to be determined. However, in principle they should be more reliable than the gas-phase CNDO/S parameters previously used.

TABLE 6: CNDO/S-Derived Properties of NMA (after Manning and Woody)[a]

transition	energy (eV)	transition dipole (D)	transition quadrupole moment (au)	magnetic transition moment (BM)
nπ*	5.63[b]	0.07	(−1.38, 0.00, 1.38)	1.19
$\pi\pi$*	6.53	3.07	(0.30, −1.17, 0.22)	N/A[c]
(nπ*−$\pi\pi$*)	N/A	0.05	(0.28, 0.00, −0.28)	N/A

[a] Coordinate system as defined in the legend to Figure 1. [b] Not the actual value calculated from CNDO/S, which was anticipated to be too low (4.06 eV). Due to an incomplete description of the location of a pair of monopoles accounting for s−p hybridization, the ground state permanent dipole moment could not be definitively computed. Two other transitions were also reported: n′π* (6.89 eV) and $\pi_+\pi$* (8.85 eV). The quadrupole moments are computed relative the center of mass and are reported as the Q_{xx}, Q_{yy}, and Q_{zz} components of the diagonalized quadrupole tensor. [c] N/A = not applicable.

Discussion

Recently,[38,47] the electronic states of amides have been studied using multiconfigurational second-order perturbation theory (CASPT2). The computed second-order vertical energies were reported to be within 0.2 eV of the experimental energies. For formamide and NMA the agreement between the experimental band maxima and the CASPT2 $\pi\pi$* transition energy is good, but for acetamide and particularly NMF the agreement is poorer than 0.2 eV. The CASPT2 $\pi\pi$* transition energy for NMF is 6.71 eV. Serrano-Andrés and Fülscher[38] discuss the experimental data, which show a broad band from 7.0−7.6 eV, with Kaya and Nagakura[13] specifically reporting peaks at 7.08, 7.16, and 7.22 eV and an obvious maximum at 7.40 eV. They argue that a 0.7 eV error in their calculation is very unlikely and suggest that the experimental spectrum should be reinterpreted to the effect that the $\pi\pi$* state is hidden on the low-energy side of the broad band. There is no suitable candidate for the origin of the band that hides the $\pi\pi$* state, and thus the lack of other intense transitions in this region does not support this interpretation.

There are several differences in methodology between the MRCI calculations presented here and the CASPT2 calculations, including basis set, the treatment of correlation, and the treatment of the interaction between Rydberg and valence states. Examination of the influence of basis set and correlation on the computed spectrum of formamide suggests that the discrepancies between the MRCI and CASPT2 calculations do not arise from either of these factors and that the most likely explanation lies in the different treatment of the interaction between Rydberg and valence states. Our approach has been to perform one state-averaged calculation with one active space that includes Rydberg orbitals. The advantage of this approach is that all states are treated equally; the disadvantage is that there may be some artificial mixing between the Rydberg and valence states. To avoid this possible artificial mixing, the protocol used in the CASPT2 calculations ignores the interaction between Rydberg and valence states. Several calculations are performed: one for the Rydberg states with an active space that includes Rydberg orbitals and one for the valence states with an active space in which the Rydberg orbitals have been deleted and completely removed from the calculation, and also it appears that separate single-root optimizations are performed for the ground state for both active spaces.

The CASPT2 results for NMF suggest that this approach is not completely satisfactory. The MRCI results are also not entirely satisfactory, with the $\pi\pi$* energies appearing to be consistently 0.3−0.6 eV too high, possibly due to artificial mixing between Rydberg and valence states. However, we

TABLE 7: Transition Properties of NMA Computed from MRCI Wave Functions[a]

calculation	transition	energy (eV)	transition dipole (D)	transition quadrupole moment (au)	magnetic transition moment (BM)
active space	nπ*	6.14	0.10	(1.23, 0.00, −1.23)	0.89
(15, 2; 16, 7)	$\pi\pi$*	7.46	2.06	(−0.78, 1.39, −0.61)	0.24
	(nπ*−$\pi\pi$*)	N/A[b]	−1.28	(3.49, 0.00, −3.49)	0.24
active space	nπ*	5.96	0.12	(0.93, 0.00, −0.93)	0.92
(15, 2; 17, 5)	$\pi\pi$*	7.62	3.37	(0.94, 1.48, −0.54)	0.32
	(nπ*−$\pi\pi$*)	N/A	−0.45	(0.00, −1.05, 1.05)	0.35

[a] For the purposes of computing the circular dichroism of proteins, the experimental transition energies observed for proteins are more appropriate than the gas-phase NMA transition energies. [b] N/A = not applicable.

TABLE 8: Permanent Properties of Electronic States of NMA Computed from MRCI Wave Functions

calculation	state	perm dipole moment (D)	perm quadrupole moment (au)
active space	ground	4.92	(7.01, −3.95, −3.06)
(15, 2; 16, 7)	nπ*	1.27	(7.28, −1.90, −5.38)
	$\pi\pi$*	6.94	(0.94, 17.51, −18.44)
active space	ground	4.59	(5.13, −3.18, −1.95)
(15, 2; 17, 5)	nπ*	1.81	(4.91, −1.02, −3.89)
	$\pi\pi$*	4.39	(8.19, −3.50, −4.69)

believe the disadvantage of this seemingly systematic error is out-weighed by the advantage of the balance and relative straightforwardness of the single state-averaged calculation. Furthermore, we speculate that the discrepancy between the MRCI results and the experimental spectra may not arise from deficiencies in the calculation. The electronic spectra of the amides might be expected to be analogous to that of ethylene, where the band maximum is thought to correspond to a nonvertical transition. If this is the case for amides, one would expect that the computed vertical energies would be higher than the experiment band locations. CASPT2 and MRCI calculations are both well-established methodologies for computing electronic excited states. Our calculations allow a comparison between the two methods and highlight a number of interesting issues concerning the electronic spectra of amides.

We have shown that MRCI calculations, based on a single state-averaged calculation with one active space that includes Rydberg orbitals, are capable of reproducing the basic features of amide electronic spectra. The Rydberg transitions are well described by both the MRCI and CASPT2[38] calculations. For acetamide and NMA, the MRCI calculations indicate $\pi 3p_\pi$ transitions with significant intensity, and as in the case with formamide, there appears to be a significant interaction between the $\pi 3p_\pi$ state and the $\pi\pi$* state. CASPT2 calculations compute Rydberg transition energies to be, on average, about 0.2 eV higher than the MRCI transition energies. The experimental data are not sufficiently precise to resolve this discrepancy. Apart from the primary amides, where oscillator strengths of between 0.05 and 0.1 are calculated for the $\pi 3p_\pi$ transition, the CASPT2 calculations do not predict any Rydberg 3s or 3p transitions with significant intensity. The MRCI calculations also predict that these transitions have small oscillator strengths, although for the secondary amides the values are about twice the CASPT2 values.

The MRCI vertical $\pi\pi$* transition energy is 0.3−0.6 eV higher than the band maxima. This difference appears to be systematic and may indicate that the treatment of the interaction between valence and Rydberg states is inadequate, or it may suggest that the band maxima correspond to nonvertical transitions. CASPT2 calculations[38] which neglect the valence−Rydberg interaction completely as being artificial appear to underestimate the $\pi\pi$* transition energy, although not in a systematic fashion. The correct treatment of the Rydberg−valence interaction clearly will be an important step in improving our understanding of the amide electronic spectra. Unfortunately, at the moment one has to choose between neglecting this interaction completely or including as we have done, with the knowledge that the MRCI technique may only get the balance between Rydberg and valence states partially correct.

Overall, both CASPT2 and MRCI methods give a qualitatively similar theoretical picture of the amide electronic spectra. The important influence of correlation effects on the amide electronic structure is clear and has been appropriately accounted for. The major differences between the calculations are the $\pi\pi$* transition energies which are underestimated by the former and overestimated by the latter and the intensity of the Rydberg $\pi 3p_\pi$ transition in several of the amide spectra. The differences are probably attributable to different and imperfect treatments of the interaction between Rydberg and valence states. This study has highlighted the importance of this interaction.

Acknowledgment. We thank the Pittsburgh Supercomputing Center for computational resources. J.D.H. thanks the Human Frontiers Science Program for a long-term fellowship. Financial support of J.D.H. by the NSF (Grant MCB-9632124), D.M.H. by the EPSRC, and C.L.B. by the NIH (GM 48807, GM 37554) is gratefully acknowledged.

References and Notes

(1) Guo, H.; Karplus, M. *J. Phys. Chem.* **1992**, *96*, 7273−7287.
(2) Dixon, D. A.; Dobbs, K. D.; Valentini, J. J. *J. Phys. Chem.* **1994**, *98*, 13435−13439.
(3) Wang, Y.; Purrello, R.; Georgiou, S.; Spiro, T. G. *J. Am. Chem. Soc.* **1991**, *113*, 6368−6377.
(4) Polavarapu, P. L.; Deng, Z.; Ewig, C. S. *J. Phys. Chem.* **1994**, *98*, 9919−9930.
(5) Chen, X. G.; Schweitzer-Stenner, R.; Krimm, S.; Mirkin, N. G.; Asher, S. A. *J. Am. Chem. Soc.* **1994**, *116*, 11141−11142.
(6) Song, S.; Asher, S. A.; Krimm, S.; Shaw, K. D. *J. Am. Chem. Soc.* **1991**, *113*, 1155−1163.
(7) Krimm, S.; Song, S.; Asher, S. A. *J. Am. Chem. Soc.* **1989**, *111*, 4290−4294.
(8) Jorgensen, W. L.; Gao, J. *J. Am. Chem. Soc.* **1988**, *110*, 4212−4216.
(9) Yu, H.-A.; Pettitt, B. M.; Karplus, M. *J. Am. Chem. Soc.* **1991**, *113*, 2425−2434.
(10) Manning, M. C.; Woody, R. W. *Biopolymers* **1991**, *31*, 569−586.
(11) Katz, J. L.; Post, B. *Acta Crystallogr.* **1960**, *13*, 624−628.
(12) Kitano, M.; Fukuyama, T.; Kuchitsu, K. *Bull. Chem. Soc. Jpn.* **1973**, *46*, 384−387.
(13) Kaya, K.; Nagakura, S. *Theoret. Chim. Acta* **1967**, *7*, 117−123.
(14) Nielsen, E. B.; Schellman, J. A. *J. Phys. Chem.* **1967**, *71*, 2297−2304.
(15) Nitzsche, L. E.; Davidson, E. R. *J. Am. Chem. Soc.* **1978**, *100*, 7201−7204.
(16) Kitano, M.; Kuchitsu, K. *Bull. Chem. Soc. Jpn.* **1974**, *47*, 631−634.
(17) Kitano, M.; Kuchitsu, K. *Bull. Chem. Soc. Jpn.* **1973**, *46*, 3048−3051.
(18) Clark, L. B. *J. Am. Chem. Soc.* **1995**, *117*, 7974−7986.
(19) Hirst, J. D.; Hirst, D. M.; Brooks, C. L. *J. Phys. Chem.* **1996**, *100*, 13487−13491.
(20) Roos, B. O.; Fülscher, M. P.; Malmqvist, P.-Å.; Merchán, M.; Serrano-Andrés, L. In *Quantum Mechanical Electronic Structure Calcula-*

tions with Chemical Accuracy; Langhoff, S. R., Ed.; Kluwer Academic Publishers: Dordrecht, The Netherlands, 1995; pp 357−438.

(21) Lindh, R.; Roos, B. O. *Int. J. Quant. Chem.* **1989**, *35*, 813−825.

(22) Peyerimhoff, S. D.; Buenker, R. J. *Theoret. Chim. Acta* **1972**, *27*, 243−264.

(23) Serrano-Andrés, L.; Merchán, M.; Nebot-Gil, I.; Lindh, R.; Roos, B. O. *J. Chem. Phys.* **1993**, *98*, 3151−3162.

(24) Hachey, M. R. J.; Bruna, P. J.; Grein, F. *J. Phys. Chem.* **1995**, *99*, 8050−8057.

(25) Merchán, M.; Roos, B. O. *Theoret. Chim. Acta* **1995**, *92*, 227−239.

(26) Merchán, M.; Roos, B. O.; McDiarmid, R.; Xing, X. *J. Chem. Phys.* **1996**, *104*, 1791−1804.

(27) Serrano-Andrés, L.; Merchán, M.; Nebot-Gil, I.; Roos, B. O.; Fülscher, M. *J. Am. Chem. Soc.* **1993**, *115*, 6184−6197.

(28) Fülscher, M. P.; Andersson, K.; Roos, B. O. *J. Phys. Chem.* **1992**, *96*, 9204−9212.

(29) Fülscher, M. P.; Roos, B. O. *Theoret. Chim. Acta* **1994**, *87*, 403−413.

(30) Chen, X. G.; Asher, S. A.; Schweitzer-Stenner, R.; Mirkin, N. G.; Krimm, S. *J. Am. Chem. Soc.* **1995**, *117*, 2884−2895.

(31) Li, Y.; Garrell, R. L.; Houk, K. N. *J. Am. Chem. Soc.* **1991**, *113*, 5895−5896.

(32) MOLPRO is a package of *ab initio* programs written by H.-J. Werner and P. J. Knowles, 1994, with contributions from J. Almlöf, R. Amos, M. J. P. Deegan, S. Elbert, C. Hampel, W. Meyer, K. Peterson, R. Pitzer, A. J. Stone, and P. R. Taylor.

(33) Werner, H.-J.; Knowles, P. J. *J. Chem. Phys.* **1988**, *89*, 5803−5814.

(34) Knowles, P. J.; Werner, H.-J. *Chem. Phys. Lett.* **1988**, *145*, 514−522.

(35) Knowles, P. J.; Werner, H.-J. *Chem. Phys. Lett.* **1985**, *115*, 259−267.

(36) Werner, H.-J.; Knowles, P. J. *J. Chem. Phys.* **1985**, *82*, 5053−5063.

(37) Møller, C.; Plesset, M. S. *Phys. Rev.* **1934**, *46*, 618−622.

(38) Serrano-Andrés, L.; Fülscher, M. P. *J. Am. Chem. Soc.* **1996**, *118*, 12190−12199.

(39) Frisch, M. J.; Trucks, G. W.; Schlegel, H. B.; Gill, P. M. W.; Johnson, B. G.; Robb, M. A.; Cheeseman, J. R.; Keith, T. A.; Petersson, G. A.; Montgomery, J. A.; Raghavachari, K.; Al-Laham, M. A.; Zakrzewski, V. G.; Ortiz, J. V.; Foresman, J. B.; Cioslowski, J.; Stefanov, B. B.; Nanayakkara, A.; Challacombe, M.; Peng, C. Y.; Ayala, P. Y.; Chen, W.; Wong, M. W.; Andres, J. L.; Replogle, E. S.; Gomperts, R.; Martin, R. L.; Fox, D. J.; Binkley, J. S.; Defrees, D. J.; Baker, J.; Stewart, J. P.; Head-Gordon, M.; Gonzalez, C.; Pople, J. A. Gaussian 94 (Revision A.1), 1995, Gaussian Inc., Pittsburgh, PA.

(40) Hehre, W. J.; Radom, L.; Schleyer, P. R.; Pople, J. A. *Ab Initio Molecular Orbital Theory*; John Wiley & Sons: New York, 1986.

(41) Dunning, T. H.; Hay, P. J. In *Modern Theoretical Chemistry*; Schaefer, H. F., Ed.; Plenum Press: New York, 1977; Vol. 3, pp 1−27.

(42) Knowles, P. J.; Werner, H.-J. *Theoret. Chim. Acta* **1992**, *84*, 95−103.

(43) Bayley, P. M.; Nielsen, E. B.; Schellman, J. A. *J. Phys. Chem.* **1969**, *73*, 228−243.

(44) Tinoco, I. *Adv. Chem. Phys.* **1962**, *4*, 113−160.

(45) Woody, R. W.; Tinoco, I. *J. Chem. Phys.* **1967**, *46*, 4927−4945.

(46) Woody, R. W. *J. Chem. Phys.* **1968**, *49*, 4797−4806.

(47) Serrano-Andrés, L.; Fülscher, M. P. *J. Am. Chem. Soc.* **1996**, *118*, 12200−12206.